"APISAT2014", 2014 Asia-Pacific International Symposium on Aerospace Technology, APISAT2014

Effect of Recession on the Re-entry Capsule Aerodynamic Characteristic

Xu Guowu*, Zhou Weijiang, Chen Bingyan, Zhan Huiling, Yang Yunjun

China Academy of Aerospace Aerodynamics, Beijing, P.R.China, 100074

Abstract

Numerical simulation and analysis of aerodynamic characteristics of Soyuz ablation shape is carried out in this paper for the adverse influence coming from recession. The result indicates that the shape change caused by the recession will increase absolute value of trim angle of attack and trim lift-drag ratio. The conclusion offers reference for the aerodynamic layout design and improve of the Soyuz re-entry capsule.

© 2015 Published by Elsevier Ltd. This is an open access article under the CC BY-NC-ND license (http://creativecommons.org/licenses/by-nc-nd/4.0/).
Peer-review under responsibility of Chinese Society of Aeronautics and Astronautics (CSAA)

Keywords: re-entry capsule; recession; trim angle of attack; trim lift-drag ratio

1. Introduction

The air environment is complicated during the re-entry of capsule. It must go through hypersonic, supersonic, transonic and subsonic flow. The aerodynamic characteristic of the re-entry capsule are variant in different flow[1,2]. In order to make the re-entry flight stable and credible, we need to forecast flow field accurately, including the aerodynamic characteristic and trim characteristic. Trim angle of attack reflects balanceable flight of re-entry capsule. And stable trim angle of attack during re-entry is needed in engineering design. During the high-speed re-entry, airflow compression makes high temperature and high pressure on ball crown surface of the re-entry capsule, so that thermo-chemical ablation is occurred in the thermal protection system. The ball crown surface will undergo recession, gradually changing the shape of the re-entry capsule, and therefore changing the aerodynamic

* Corresponding author. Tel.: +86-010-68743745.
    E-mail address: elexgw@163.com

characteristic and trim characteristic of the vehicle.

There are some research about re-entry capsule at home[3-10], while study on the changes of aerodynamic characteristic caused by recession is rarely seen. However, impact of recession on the ORION Crew Exploration Vehicle(CEV) aerodynamics is analyzed abroad[11-14]. Numerical simulation of Soyuz re-entry capsule is carried out in this paper. Soyuz is blunt body aircraft, and when the large end is put forward, axial force is larger than normal force, and therefore the lift mainly comes from axial force, so that the lift is positive when the angle of attack is minus. The aerodynamic characteristic of Soyuz is calculated and analyzed in this paper, and also the impact of recession is researched.

2. Numerical method

Compressible flow and viscous gas kinetic equation is used as flow field control equation:

$$\frac{\partial}{\partial t}\int_{\Omega}\boldsymbol{Q}\mathrm{d}V + \int_{\partial\Omega}\boldsymbol{F}\cdot\hat{\boldsymbol{n}}\mathrm{d}S = \int_{\partial\Omega}\boldsymbol{G}\cdot\hat{\boldsymbol{n}}\mathrm{d}S \tag{1}$$

$$\boldsymbol{Q}=\begin{pmatrix}\rho\\\rho u\\\rho v\\\rho w\\E\end{pmatrix},\qquad \boldsymbol{F}=\begin{pmatrix}\rho u\\\rho u^2+p\\\rho uv\\\rho uw\\u(E+p)\end{pmatrix}\hat{\boldsymbol{i}}+\begin{pmatrix}\rho v\\\rho vu\\\rho v^2+p\\\rho vw\\v(E+p)\end{pmatrix}\hat{\boldsymbol{j}}+\begin{pmatrix}\rho w\\\rho wu\\\rho wv\\\rho w^2+p\\w(E+p)\end{pmatrix}\hat{\boldsymbol{k}} \tag{2}$$

$$\boldsymbol{G}=\begin{pmatrix}0\\\tau_{xx}\\\tau_{xy}\\\tau_{xz}\\u\tau_{xx}+v\tau_{xy}+w\tau_{xz}-q_x\end{pmatrix}\hat{\boldsymbol{i}}+\begin{pmatrix}0\\\tau_{yx}\\\tau_{yy}\\\tau_{yz}\\u\tau_{yx}+v\tau_{yy}+w\tau_{yz}-q_y\end{pmatrix}\hat{\boldsymbol{j}}+\begin{pmatrix}0\\\tau_{zx}\\\tau_{zy}\\\tau_{zz}\\u\tau_{zx}+v\tau_{zy}+w\tau_{zz}-q_z\end{pmatrix}\hat{\boldsymbol{k}} \tag{3}$$

Where ρ is density, p is pressure, u、v、w is velocity of three direction, E is total energy:

$$E=\frac{p}{\gamma-1}+\frac{1}{2}\rho\left(u^2+v^2+w^2\right) \tag{4}$$

$$\boldsymbol{\tau}=\mu\begin{bmatrix}2u_x & u_y+v_x & u_z+w_x\\u_y+v_x & 2v_y & v_z+w_y\\u_z+w_x & v_z+w_y & 2w_z\end{bmatrix}-\frac{2}{3}\mu(u_x+v_y+w_z)\boldsymbol{I} \tag{5}$$

Grid center of finite volume method is used to disperse computational domain, and Roe format is used to compute inviscid flux, and entropy correction is used to avoid non-physical solution. In order to achieve high-order accuracy, least square method is used to obtain gradient distribution in the unit. Time stepping adopts LU-SGS method, which is foremost introduced by Jameson and Yoon.

3. Results and analysis

3.1. Configuration changing caused by recession

Soyuz re-entry capsule recession configurations in different trajectory are obtained by material ablation calculating. Figure 1 shows contrast of original shape and recessed shape of Soyuz at re-entry terminal (Ma=5、H=40km), where the recession is most serious. There is an obvious disfigurement in the large end, which is deep windward and shallow leeward.
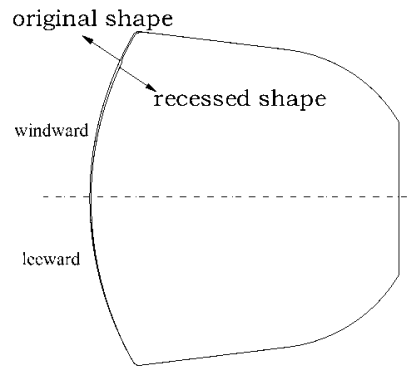
Fig. 1. Contrast of before recession and after recession configuration of re-entry capsule(symmetry plane).

3.2. Computation mesh

Structural mesh is used for numerical calculation, shown in Figure 2. Mesh refinement is adopted in the disfigurement area in order to modeling the recessed shape accurately
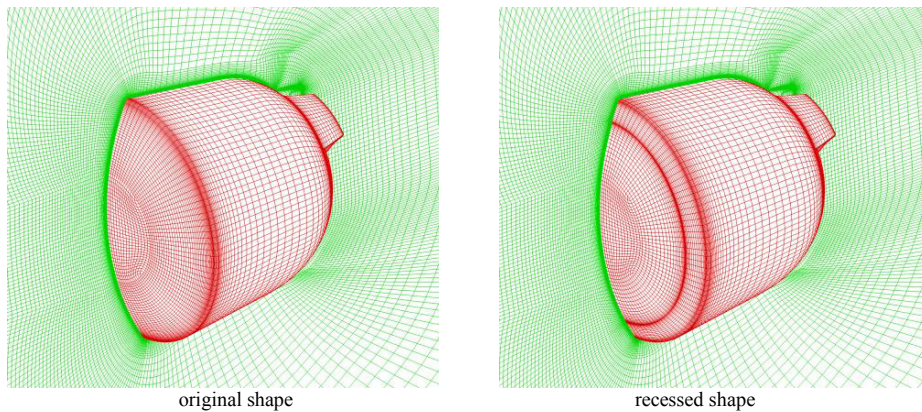

original shape   recessed shape

Fig. 2. Structural mesh.

3.3. Computed result

The aerodynamic forces and moments for Ma=5, H=40km are given in this section, shown in figure 3, to provide an overview of how the aerodynamic change with recession, where C_A is axial force coefficient, C_N is normal force coefficient, C_{MZG} is pitching moment coefficient. There is little difference between original and recessed C_A. The differences in C_N and *L/D* are more evident, but is still very small. Absolute value of C_N increases slightly and *L/D* decreases appreciably due to recession. The pitching moment, unlike the forces, shows a clear difference between original shape and recessed shape. The recession has an effect of down pitching moment so as to increase absolute value of trim angle of attack. A greater variation occurs in longitudinal center of pressure coefficient X_{cp}, which moves forth due to recession, and as absolute value of angle of attack decreases, the difference in X_{cp} increases
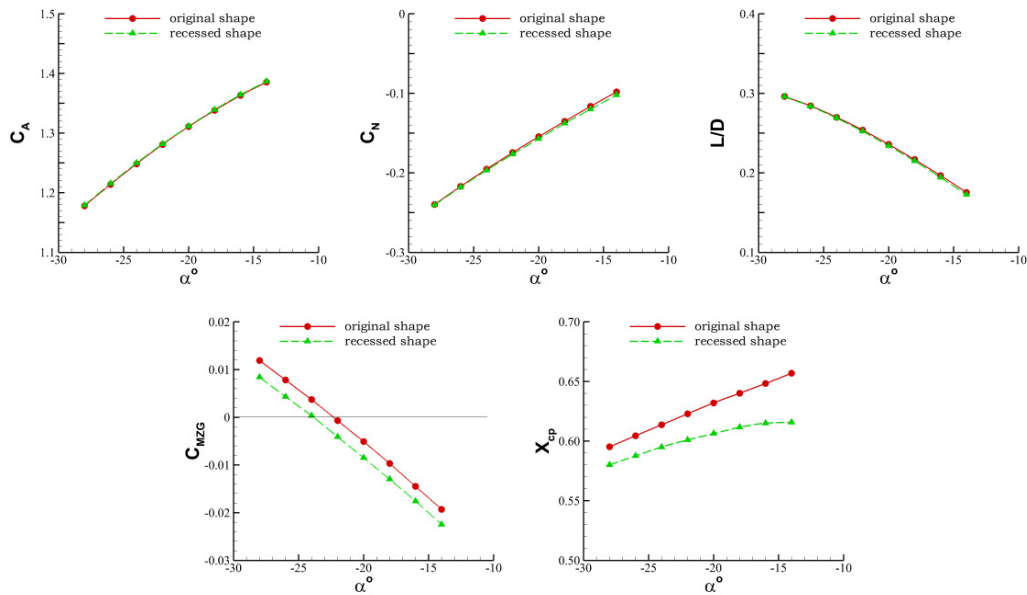
Fig. 3. Aerodynamic forces and moments.

Table 1 shows the contrast of trim angle of attack and trim *L/D* of original shape and recessed shape. Based on the results from table 1, the absolute value of trim angle of attack increases about 1.6° and trim *L/D* increases about 0.0116 due to the recession.

Table 1. Comparison of trim characteristic.

	Original shape	Recessed shape
Trim α	-22.3°	-23.9°
Trim *L/D*	0.2563	0.2679

3.4. Compare with reference

CEV and Soyuz are both blunt body aircrafts. they have same aerodynamic mechanism, and the lift mainly comes from axial force. According to reference [11] Soyuz and CEV also have same changes in the law of trim characteristic. Figure 4 show the impact on delta trim angle of attack and delta trim *L/D* along the trajectory due to recession. Note that the recession increases from right to left. The effect of recession is to increase absolute value of the trim angle of attack and the trim *L/D*, with $\Delta\alpha$=1.1°and Δ(*L/D*)=0.0155 for the Ma=5 condition. The qualitative facts of reference [11] compare well with the results of Soyuz in this paper.
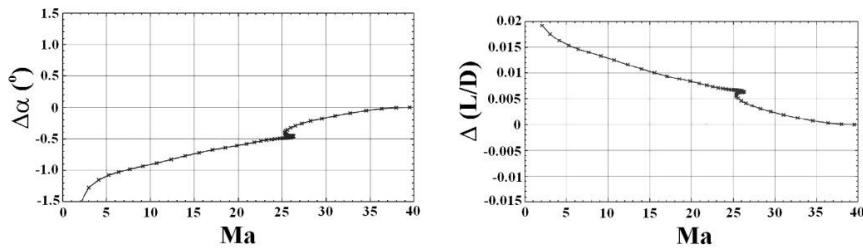
Fig. 4. Recession effect on trim angle of attack and trim L/D.

3.5. Mechanism analysis

Figure 5 shows the comparison the symmetric plane pressure of original shape vs. the symmetric plane pressure of recessed shape for the Ma=5,H=40km,α=-20° condition. Jumping phenomenon of pressure is obviously seen on large end of recessed shape, while pressure of other units compares well with original shape. The change of aerodynamic force, therefore, is mainly coming from the change of large end surface pressure. As a visual representation, the pressure change from windward of large end makes a pitching up moment, while the pressure change from leeward of large end makes a pitching down moment. Figure 6 shows the symmetric plane nephogram of mach number for the Ma=5, H=40km,α=-20° condition. The disfigurement in windward of large end is in subsonic flow, while disfigurement in leeward of large end is in supersonic flow. As a result of that, the impact of pressure change from windward of large end is much smaller than from leeward of large end. Therefore, the pressure change makes a pitching down moment and increases absolute value of the trim angle of attack.
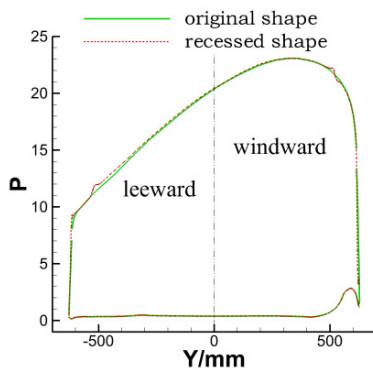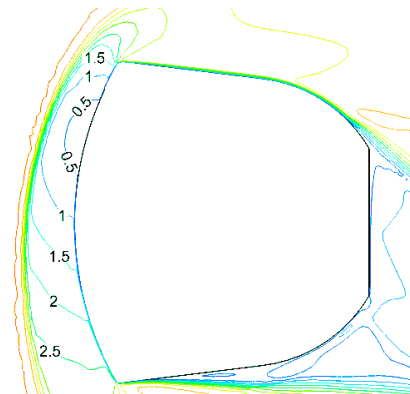

Fig. 5. Comparison of surface pressure(α=-20°).

Fig. 6. Nephogram of mach number(α=-20°).

In order to quantitative analyze, the re-entry capsule is divided into three units: windward of large end, leeward of large end and afterbody, shown in figure 7. Aerodynamic coefficient of each unit is contrasted for the Ma=5,H=40km,α=-22.3° condition, shown in table 2, where α=-22.3° is the trim angle of attack of original shape. Referring to the results in table 2 the aerodynamic coefficient from afterbody has no dispersion (ΔC_A=0, ΔC_N=0, ΔC_{MZG}=0), meaning the change of aerodynamic force is independent of afterbody. Normal force coefficient from windward of large end is increasing, making a tiny pitching up moment (ΔC_{MZG}=0.0002). Normal force coefficient from leeward of large end is decreasing and axial force coefficient is increasing, making a pitching down moment (ΔC_{MZG}=-0.0036). Therefore, the pitching down moment of recessed shape is mostly coming from the pressure change of leeward of large end.
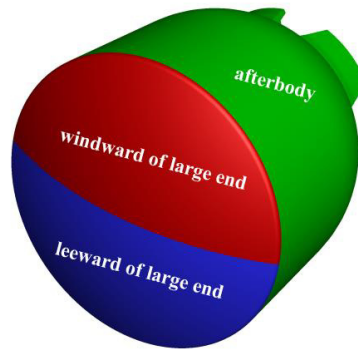
Fig. 7. Schematics of re-entry capsule unit.

Table 2. Comparison of unit aerodynamic coefficient (Ma=5,H=40km,α=-22.3°).

		Windward of large end	Leeward of large end	afterbody	Re-entry capsule
C_A	original	0.7420	0.5105	0.0144	1.2668
	recessed	0.7420	0.5208	0.0144	1.2771
	ΔC_A	0	0.0103	0	0.0103
C_N	original	-0.1786	0.1021	-0.1020	-0.1785
	recessed	-0.1773	0.0997	-0.1020	-0.1796
	ΔC_N	0.0013	-0.0024	0	-0.0011
C_{MZG}	original	0.0804	-0.0802	-0.0002	0
	recessed	0.0806	-0.0838	-0.0002	-0.0034
	ΔC_{MZG}	0.0002	-0.0036	0	-0.0034

Figure 8 shows the resultant force vector diagram of above-mentioned result. The intersection point of the resultant force F and axis makes the longitudinal center of pressure coefficient X_{cp}, and the included angle θ can be expressed as:

$$\theta = \arctan \left| \frac{C_N}{C_A} \right| \tag{6}$$

Supposing the resultant force of original shape and recessed shape is F_1 and F_2, and the included angle is θ_1 and θ_2, longitudinal center of pressure is X_{cp1} and X_{cp2}. Based on above-mentioned result, X_{cp2} is in front of X_{cp1}. Referring to table 2 and formula of θ it can be gained that: θ_1=8.021°, θ_2=8.005, so that $\theta_2<\theta_1$. Besides, the resultant force F_1 goes through centroid X_{cg} because of condition: α=-22.3°, which is the trim angle of attack of original shape. As a result, the location of F_2 and X_{cg} is just shown as figure 8, from which we can obviously see that the resultant force of recessed shape F_2 makes a pitching down moment, so as to increase the absolute value of trim angle of attack and trim *L/D*.
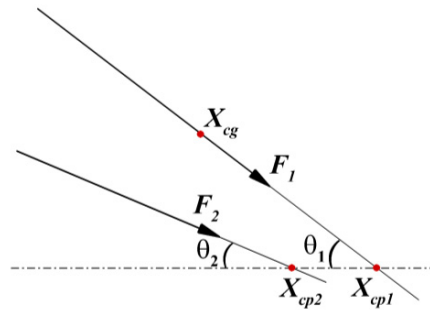
Fig. 8. Resultant force vector diagram.

4. Conclusion

Recession of re-entry capsule primarily makes a pitching down moment, so that the effect of recession is to increase absolute value of the trim angle of attack and trim *L/D*. And the pitching down moment of recessed shape of Soyuz re-entry capsule is mainly coming from the pressure change of leeward of large end. Soyuz and CEV have same changes in the law of trim characteristic, and recessed shape of them also have same changes in trends. The conclusion in this paper offers reference for the aerodynamic layout design and improve of the Soyuz re-entry capsule.

References

[1] Ji Chu-qun, Zhou Wei-jiang. A numerical simulation of aerodynamic characters for bell capsule [J]. Spacecraft Recovery & Remote Sensing, 2000, 18(1):32-37.
[2] Chen He-wu. Wind-tunnel test analysis on hypersonic aerodynamic characteristics of returnable module [J]. Spacecraft   Engineering, 2008, 17(5):77-81.
[3] Zhou Wei-jiang. Numerical simulation of unsteady transonic flow around a free oscillating re-entry vehicle [J]. Acta Aerodynamic Sinica, 2000, 18(1):46-51.
[4] Zhao Meng-xiong. Ablative thermal protection of capsule type re-entry vehicle [J]. Aerodynamic Experiment And Measurement & Control, 1996, 10(3):1-9.
[5] Zhao Meng-xiong. The aerodynamic and aerothermodynamic circumstances of capsule type re-entry vehicle [J]. Aerodynamic Experiment And Measurement & Control, 1995, 9(4):1-7.
[6] Zhao Meng-xiong. The aerodynamic heating distributions of capsule type re-entry vehicle [J]. Aerodynamic Experiment And Measurement & Control, 1996, 10(1):1-8.
[7] Zhao Meng-xiong. The trim aerodynamic characteristics of capsule type re-entry vehicle [J]. Aerodynamic Ex-periment And Measurement & Control, 1995, 9(1):1-9.
[8] Zhu Guang-chen. Improvement on protecting technology against the reentry and landing mechanical environment of manned spacecraft return module [J]. Spacecraft Recovery & Remote Sensing, 2010, 31(5):9-15.
[9] Yang Zai-shan. The configuration and adrodynamic characteristics of manned re-entry capsules [J]. Aero-dynamic Experiment And Measurement & Control, 1996, 10(4):12-18.
[10] Wang An-ling, Gui Ye-wei, Geng Xiang-ren, et al. Study on uncertainty bands of aerodynamically heating rate and material performance in thermal protection for spaceship capsule [J]. Journal of Engineering Thermophysics, 2005, 26(5):862-864.
[11] Kinney D J. Impact of TPS recession on the orion CEV aerodynamics [C]. 47th AIAA Aerospace Sciences Meeting Including The New Horizons Forum and Aerospace Exposition, 5-8 January 2009, Orlando, Florida, AIAA 2009-1102.
[12] Kinney D J. Development of the orion crew exploration vehicle's aerothermal database using a combination of high fidelity CFD and engineering level methods[C]. 47th AIAA Aerospace Sciences Meeting Including The New Horizons Forum and Aerospace Exposition, 5-8 January 2009, Orlando, Florida, AIAA 2009-1100.
[13] Bibb K L, McDaniel R. Aerodynamic analysis of sim-ulated heat shield recession for the orion command module[C]. 46th AIAA Aerospace Sciences Meeting and Exhibit, 7-10, January 2008, Reno, Nevada, AIAA 2008-356.
[14] Titov E V, Anderson B P. Simulation of heat loads on the CEV orion compression pads during reentry[C]. 42nd AIAA Thermophysics Conference, 27-30 June 2011, Honolulu, Hawaii, AIAA 2011-3320.